Joint Active and Passive Beamforming for IRS-aided Wideband Dual-Function Radar-Communications

Tong Wei, Linlong Wu, Kumar Vijay Mishra, Bhavani Shankar M. R.
Interdisciplinary Centre for Security, Reliability and Trust (SnT), University of Luxembourg
email: {tong.wei@, linlong.wu@, kumar.mishra@ext., bhavani.shankar@}uni.lu

***Abstract*—In this paper, the problem of joint active and passive beamforming design for intelligent reflecting surface (IRS) aided wideband dual-function radar and communication (DFRC) is investigated. Specifically, we consider jointly designing the radar receive filter, frequency-dependent beamforming matrices and IRS phase shifts to maximize the average radar SINR and the minimal communication SINR among all users, simultaneously. However, the resulting problem comprises a maximin objective function, constant modulus and power constraints, and is highly nonconvex. To this end, within the alternating maximization (AM) framework, an iterative method judiciously integrates the alternating direction method of multipliers (ADMM), Riemannian steepest descent (RSD) and Dinkelbach's method to tackle the problem. Numerical experiments demonstrate that the proposed method for IRS-aided DFRC can achieve better performance for both radar and communication compared with the No-IRS case.**

***Index Terms*—Alternating maximization, Dual-function radar-communications, intelligent reflecting surfaces, OFDM.**

I. Introduction

Intelligent reflecting surface (IRS) which consists of many low-cost reconfigurable elements with the ability to control the phase of the impinging signal, draws great research interests recently [1–3]. Due to the near passive property and low cost, compared with the conventional relay scheme, IRS can be massively deployed to improve the wireless propagation without extra energy consumption [4, 5]. Leveraging on these advantages, IRS shows immense potential to be integrated into the wireless communications, MIMO radar and joint radar communications (JRC) systems [6–11].

Noted that the next generation wireless communication system is expected to provide the stable data transmission and hence the better quality of service (QoS). Hence, in order to reach the intelligent spectrum control, IRS is first deployed in wireless communication system [12–16]. For example, in [13], IRS is used to compensate the end-to-end path loss, i.e. transmitter-IRS and IRS-receiver channels. Then, the transmit power from the base station is minimized while guaranteeing a minimum signal-to-interference-plus-noise ratio (SINR) for each user. To acquire the channel state information (CSI), in [14], the authors decompose the channel into multiple subchannels, each of which is then estimated via multi-round pilot training. Utilizing the reconstructed CSI, both the active and passive beamforming are well designed to maximize the effective mutual information.

Besides, IRS can be also integrated into radar systems to enhance the performance of detection and estimation [8, 9, 17–19]. In [8], compared with radar-only system, the IRS-aided radar system can provide an additional echo from the target and thereby improve the probability of detection. Then, in [17], to improve the intensity of return signal, IRS is closely deployed to the receive antennas of MIMO radar. Meanwhile, the signal-to-noise ratio (SNR) can be maximized via devising the phase shift of reflecting elements. In [19], the authors propose the novel NLoS radar surveillance model with the assistance of a single IRS. To further expand the coverage region, IRS should be deployed in the suitable position to build the line-of-sight (LoS) path between transmitter and receiver.

Recently, joint radar and communication (JRC) system which can share both the hardward and spectrum resources has been widely investigated [20, 21]. Meanwhile, due to the flexibility of multi-beam control, IRS is also utilized in dual-function radar communication (DFRC) to enhance the ability of sensing and/or communications [10, 11, 22, 23]. For example, in [22], the passive and active beamforming are jointly devised for the IRS-aided DFRC to enhance the radar detection performance while ensuring the single-user signal-to-noise ratio (SNR). Then, in [11], the multiple transmit beams of DFBS are aligned to the target directions. Meanwhile, with the assistance of IRS, the multi-user interference (MUI) is eliminated to guarantee the quality of service (QoS). However, in this scheme, IRS can be only used to improve the communication performance. Notice that the above mentioned IRS-assisted DFRC systems emit the narrow-band signals while limit the achievable rates.

Different from the previous schemes [22, 23], in this paper, the focus lies on integrating IRS into wideband OFDM-DFRC system in which both the LoS and NLoS path are considered. Further, the work considers both radar and communication metrics simultaneously. By jointly designing the radar receive filter, active beamforming (i.e., transmit precoding matrix) and passive beamforming (i.e., IRS phase-shift matrix), the radar SINR and the minimal communication SINR are maximized. The resulting optimization problem is solved by the alternating maximization (AM) framework. Numerical results are provided to illustrate the effectiveness and superiority of the proposed design approach.

Notations: Vectors and matrices are denoted by lower case boldface letter and upper case boldface letter, respectively. $(\cdot)^T$, $(\cdot)^*$ and $(\cdot)^H$ denote denote the operations of transpose, conjugate, and Hermitian transpose, respectively. $\mathbf{I}_L$ denotes the $L \times L$ identity matrix. Finally, $\|\cdot\|_2$ and $\|\cdot\|_F$ represent the ℓ_2-norm and Frobenius-norm, respectively.

II. Signal Model

Consider an IRS-assisted wideband OFDM-DFRC system consisting of a N_t-antenna dual-function transmitter, a N_r-antenna radar receiver and a single IRS comprising N_m reflecting elements, and aiming to detect a target in presence of Q clutters while simultaneously serving U single-antenna downlink (DL) users. Herein, the transmitter and receiver are composed by uniform linear array (ULA) and closely deployed into the dual-function base station (DFBS). Meanwhile, we consider both the direct and indirect links (i.e., LoS and NLoS) for radar and communication. The transmit signal is composed of OFDM symbols, having the symbol duration $\triangle t$ and modulated to spread over K subcarriers. Denoting the normalized transmit data symbol at the k-th subcarrier as $\mathbf{s}_k = [s_{k,1}, \cdots, s_{k,U}]^T \in \mathbb{C}^{U\times 1}$, where $k = 1, \cdots, K$ and $\mathbb{E}\{\mathbf{s}_k\mathbf{s}_k^H\} = \mathbf{I}_U$. To overcome spatial wideband effect known as beam squint [24], we utilize the frequency-dependent digital beamforming $\mathbf{F}_k \in \mathbb{C}^{N_t\times U}$ to precode the data symbol such that the signal $\mathbf{F}_k\mathbf{s}_k \in \mathbb{C}^{N_t\times 1}$ is transmitted on the k-th subcarrier. By utilizing the N_t K-point inverse fast Fourier transform (IFFT), the transmit baseband signal can be given by

$$\mathbf{x}(t) = \sum_{k=1}^{K} \mathbf{F}_k\mathbf{s}_k e^{\jmath 2\pi f_k t}, \tag{1}$$

where t denotes the time instant, $f_k = (k-1)\triangle f$ denotes the baseband frequency at the k-th subcarrier with $\triangle f$ being the frequency step of OFDM signaling. To guarantee the orthogonality of each subcarriers, the frequency step-size is set as $\triangle f = 1/\triangle t$. On the other hand, for wideband DFRC, the transmit power should meet the system requirement, i.e.,

$$\|\mathbf{F}_k\|_F^2 \le P_k, \tag{2}$$

where P_k denotes the maximum power assigned to the k-th subcarrier.

A. Radar Model

We denote the frequency-dependent steering vectors of dual-function transmitter, radar receiver and m-th IRS, respectively, as

$$\begin{aligned}
\mathbf{a}_t(\theta, f_k) &= [1, e^{-jv(\theta,f_k)}, \cdots, e^{-j(N_t-1)v(\theta,f_k)}]^T,\\
\mathbf{a}_r(\theta, f_k) &= [1, e^{-jv(\theta,f_k)}, \cdots, e^{-j(N_r-1)v(\theta,f_k)}]^T,\\
\mathbf{b}_m(\theta, f_k) &= [1, e^{-jv(\theta,f_k)}, \cdots, e^{-j(N_m-1)v(\theta,f_k)}]^T,
\end{aligned}$$

where $m = 1\cdots, M$ and $v(\theta, f_k) = 2\pi(f_k + f_c)(\frac{d\sin(\theta)}{c})$. After sampling the signal and applying K-point FFT, the radar receive signal at the k-th subcarrier is given by

$$\begin{aligned}
\mathbf{Y}(f_k) =& \mathbf{A}_k\mathbf{F}_k\mathbf{s}_k + \boldsymbol{E}_k(\boldsymbol{\Phi})\mathbf{F}_k\mathbf{s}_k\\
&+ \widetilde{\mathbf{A}}_k\mathbf{F}_k\mathbf{s}_k + \widetilde{\boldsymbol{E}}_k(\boldsymbol{\Phi})\mathbf{F}_k\mathbf{s}_k + \mathbf{n}_r(f_k)
\end{aligned} \tag{3}$$

where $\mathbf{A}_k = \alpha_1\mathbf{a}_r^H(\theta_{d,t}, f_k)\mathbf{a}_t^H(\theta_{d,t}, f_k)$ denotes the target response matrix for direct path (i.e., Tx- target-Rx) and $\boldsymbol{E}_k(\boldsymbol{\Phi}) = \mathbf{E}_k\boldsymbol{\Phi}\mathbf{G}_k + \mathbf{D}_k\boldsymbol{\Phi}\mathbf{B}_k + \mathbf{D}_k\boldsymbol{\Phi}\mathbf{W}_k\boldsymbol{\Phi}\mathbf{G}_k$ denotes the indirect path (i.e., Tx-IRS-target-Rx, Tx-target-IRS-Rx and Tx-target-IRS-target-Rx), respectively, α_1 is the corresponding direct path gain, $\mathbf{G}_k$, $\mathbf{W}_k$, $\mathbf{D}_k$, $\mathbf{B}_k$ and $\mathbf{E}_k$ denote the channel matrix between Tx-IRS, IRS-IRS, IRS-Rx, Tx-target-IRS, IRS-target-Rx, respectively, and $\boldsymbol{\Phi}$ denotes the phase shift matrix of IRS. Similarly, $\widetilde{\mathbf{A}}_k$ and $\widetilde{\boldsymbol{E}}_k$ denote the clutter response matrix for direct path and indirect path, respectively, wherein the steering vectors and angles are omitted due to the limited space[1]. Based on (3), we can define the average SINR of radar over all subcarriers

$$\mathrm{SINR}_r = \frac{\sum_{k=1}^{K}|\mathbf{w}^H(\mathbf{A}_k + \boldsymbol{E}_k(\boldsymbol{\Phi}))\mathbf{F}_k\mathbf{s}_k|^2}{\sum_{k=1}^{K}|\mathbf{w}^H(\widetilde{\mathbf{A}}_k + \widetilde{\boldsymbol{E}}_k(\boldsymbol{\Phi}))\mathbf{F}_k\mathbf{s}_k|^2 + K\sigma_r^2\mathbf{w}^H\mathbf{w}}, \tag{4}$$

where $\mathbf{w}$ the receive filter bank and σ_r^2 denotes the noise power of radar at each subcarrier.

B. Communication Model

Denote the channel state information (CSI) matrix from transmitter to all users at k-th subcarrier as $\mathbf{H}_k \in \mathbb{C}^{U\times N_t}$. Notice that the CSI can be estimated and hence we assume that it is known. The received baseband signal of all the user can be expressed as

$$\mathbf{Y}_k(t) = \mathbf{H}_k\mathbf{F}_k\mathbf{s}_k e^{\jmath 2\pi f_k t} + \widetilde{\mathbf{H}}_k\boldsymbol{\Phi}\mathbf{G}_k\mathbf{F}_k\mathbf{s}_k e^{\jmath 2\pi f_k t} + \mathbf{n}_{c,k}(t). \tag{5}$$

Sampling the signal (5) of symbol duration and applying K-point DFT, the receive signal of the u-th user at k-th subcarrier is given by

$$\begin{aligned}
\mathbf{Y}_u(f_k) =& \mathbf{h}_{u,k}^T\mathbf{f}_{k,u}s_{k,u} + [\tilde{\mathbf{h}}_{u,k}^T\boldsymbol{\Phi}\mathbf{G}_k\mathbf{f}_{k,u}s_{k,u}\\
&+ \sum_{i\neq u}\mathbf{h}_{u,k}^T\mathbf{f}_{k,i}s_{k,i} + \sum_{i\neq u}\tilde{\mathbf{h}}_{u,k}^T\boldsymbol{\Phi}\mathbf{G}_k\mathbf{f}_{k,i}s_{k,i}] + \mathbf{n}_k(u).
\end{aligned} \tag{6}$$

where $\tilde{\mathbf{h}}_{u,k} \in \mathbb{C}^{N_m\times 1}$ denotes the channel between the u-th user and IRS, $\mathbf{f}_{k,u}$ denotes the u-th column of $\mathbf{F}_k$ and $\mathbf{n}_k(u)$ denotes the noise of u-th user. According to (6), the average signal power of the u-th user over all K subcarriers can be expressed as

$$P_u = \sum_{k=1}^{K}\| \underbrace{(\mathbf{h}_{u,k}^T + \sum_{m=1}^{M}\mathbf{h}_{u,m,k}^T\boldsymbol{\Phi}_m\mathbf{G}_{m,k})}_{\mathbf{z}_{k,u}(\boldsymbol{\Phi})}\mathbf{F}_k\boldsymbol{\Lambda}_u\|_2^2, \tag{7}$$

where $\boldsymbol{\Lambda}_u$ is the diagonal selection matrix with only the u-th element being one and the rest being zero. Meanwhile, the average power of multiuser interference (MUI) at the u-th user is

$$P_{MUI} = \sum_{k=1}^{K}\|\mathbf{z}_{k,u}(\boldsymbol{\Phi})\mathbf{F}_k\bar{\boldsymbol{\Lambda}}_u\|_2^2, \tag{8}$$

where $\bar{\boldsymbol{\Lambda}}_u$ is the diagonal matrix with only the u-th diagonal element being zero and the rest being one. Then, the SINR at the u-th users is directly given by

$$\mathrm{SINR}_u = \frac{\sum_{k=1}^{K}\|\mathbf{z}_{k,u}(\boldsymbol{\Phi})\mathbf{F}_k\boldsymbol{\Lambda}_u\|_2^2}{\sum_{k=1}^{K}\|\mathbf{z}_{k,u}(\boldsymbol{\Phi})\mathbf{F}_k\bar{\boldsymbol{\Lambda}}_u\|_2^2 + K\sigma_c^2}, \tag{9}$$

[1]Hereafter, all angles of arrival/departure are measured w.r.t the array broadside direction and are positive when moving clockwise .

where σ_c^2 denotes the noise power of communication user which is constant over all subcarriers.

C. Problem Formulation

In order to improve both the sensing and communication performance, the radar SINR and the minimal communication SINR among all users should be maximized simultaneously. Mathematically, the optimization problem is formulated as

$$\begin{aligned} \underset{\mathbf{w},\mathbf{\Phi},\mathbf{F}_k}{\text{maximize}} \quad & \text{SINR}_r + \min_u\{\text{SINR}_u\} \\ \text{subject to} \quad & \|\mathbf{F}_k\|_F^2 \le P_k, \forall k \\ & |\mathbf{\Phi}(i,i)| = 1, \forall i, \end{aligned} \tag{10}$$

where P_k denotes the maximal transmit power at k-th subcarrier. Then, problem (10) can be equivalently reformulated as

$$\begin{aligned} \underset{t,\mathbf{w}_p,\mathbf{\Phi}_m,\mathbf{F}_k}{\text{maximize}} \quad & \text{SINR}_r + t \\ \text{subject to} \quad & \text{SINR}_u \ge t, \forall u \\ & \|\mathbf{F}_k\|_F^2 \le P_k, \forall k \\ & |\mathbf{\Phi}(i,i)| = 1, \forall i, \end{aligned} \tag{11}$$

where t denotes the auxiliary variable of communication SINR threshold. Problem (11) which consists of fractional quartic objective function, constant modulus and difference of convex (DC) constraints, is highly nonconvex. To tackle problem (11), an alternating maximization (AM) based approach will be devised in the sequel.

III. Optimization method

Within the AM framework, at each iteration, we will solve four subproblems of problem (11). For each subproblem, it will be further solved iteratively.

1. Update of receive filter $\mathbf{w}$

For the given transmit beamforming $\mathbf{F}_k$ and phase-shift $\mathbf{\Phi}$, the subproblem w.r.t receive filter bank $\mathbf{w}$ can be expressed as

$$\underset{\mathbf{w}}{\text{maximize}} \ \frac{\mathbf{w}^H\mathbf{\Upsilon}_t\mathbf{w}}{\mathbf{w}^H\mathbf{\Upsilon}_c\mathbf{w} + K\sigma_r^2\mathbf{w}^H\mathbf{w}}, \tag{12}$$

where

$$\begin{aligned} \mathbf{\Upsilon}_t &= \sum_{k=1}^{K}(\mathbf{A}_k + \boldsymbol{E}_k(\mathbf{\Phi}))\mathbf{F}_k\mathbf{F}_k^H(\mathbf{A}_k + \boldsymbol{E}_k(\mathbf{\Phi}))^H, \\ \mathbf{\Upsilon}_c &= \sum_{k=1}^{K}(\widetilde{\mathbf{A}}_k + \widetilde{\boldsymbol{E}}_k(\mathbf{\Phi}))\mathbf{F}_k\mathbf{F}_k^H(\widetilde{\mathbf{A}}_k + \widetilde{\boldsymbol{E}}_k(\mathbf{\Phi}))^H. \end{aligned} \tag{13}$$

Noted that problem (12) is different from the conventional the minimum variance distortionless response (MVDR) problem due to the summation matrix $\mathbf{\Upsilon}_t$. Hence, we can not obtain the close-form solution directly. Then, the Charnes-Cooper transformation can be used to reformulate problem (12) as

$$\begin{aligned} \underset{\mathbf{w}}{\text{minimize}} \quad & \mathbf{w}^H\widetilde{\mathbf{\Upsilon}}_c\mathbf{w} \\ \text{subject to} \quad & \mathbf{w}^H\mathbf{\Upsilon}_t\mathbf{w} = 1 \end{aligned} \tag{14}$$

where $\widetilde{\mathbf{\Upsilon}}_c = \mathbf{\Upsilon}_c + K\sigma_r^2\mathbf{I}$. It is seen that problem (14) consists of the complex-valued homogeneous QCQP which is nonconvex due to the quadratic equality constraint. Then, the semidefinite relation (SDR) is used to reformulated it as

$$\begin{aligned} \underset{\mathbf{W}}{\text{minimize}} \quad & \text{Tr}(\widetilde{\mathbf{\Upsilon}}_c\mathbf{W}) \\ \text{subject to} \quad & \mathbf{W} \succeq \mathbf{0}, \\ & \text{Tr}(\mathbf{\Upsilon}_t\mathbf{W}) = 1. \end{aligned} \tag{15}$$

Based on [25], the optimal solution $\mathbf{W}^\star$ for problem (15) is rank-1, and hence the SDR is tight. Therefore, a solution of problem (14) can be obtained as: $\mathbf{W}^\star = \mathbf{w}^\star\mathbf{w}^{\star H}$.

2. Update of precoding matrices $\mathbf{F}_k$

With the fixed t, $\mathbf{w}_p$ and $\mathbf{\Phi}_\mathbf{m}$, the corresponding optimization problem can be written as

$$\begin{aligned} \underset{\boldsymbol{f}\in\mathbb{C}^{KN_tU\times 1}}{\text{maximize}} \quad & \frac{\boldsymbol{f}^H\mathbf{\Xi}_t\boldsymbol{f}}{\boldsymbol{f}^H\mathbf{\Xi}_c\boldsymbol{f} + K\sigma_r^2\mathbf{w}_p^H\mathbf{w}_p} \\ \text{subject to} \quad & \|\mathbf{V}_k\boldsymbol{f}\|_2^2 \le P_k, \forall k, \\ & \frac{\boldsymbol{f}^H\mathbf{R}_u\boldsymbol{f}}{\boldsymbol{f}^H\bar{\mathbf{R}}_u\boldsymbol{f} + K\sigma_c^2} \ge t, \forall u, \end{aligned} \tag{16}$$

where $\boldsymbol{f} = [\text{vec}(\mathbf{F}_1)^T, \cdots, \text{vec}(\mathbf{F}_K)^T]^T$, $\mathbf{V}_k$ denotes the selection matrix to extract k-th interval of $\boldsymbol{f}$. Due to space limitation, we omit the the detailed expression of semidefinite matrices $\mathbf{\Xi}_t$, $\mathbf{\Xi}_c$, $\mathbf{R}_u$ and $\bar{\mathbf{R}}_u$ which can be directly derived from (4) and (9). Noted that for the function $f(\mathbf{x}) = \mathbf{x}^H\mathbf{H}\mathbf{x}$, the following inequality is always satisfied

$$f(\mathbf{x}) \ge 2\Re(\mathbf{x}_n^H\mathbf{H}\mathbf{x}) - f(\mathbf{x}_n), \tag{17}$$

where $\mathbf{H}$ is semidefinite Hermitian matrix, $\mathbf{x}_n$ denotes the current point and the equality holds if and only if $\mathbf{x} = \mathbf{x}_n$.

Based on above inequality, we can linearize and reformulate the objective function and constraint of problem (16) as

$$\begin{aligned} \underset{\boldsymbol{f}}{\text{maximize}} \quad & \frac{2\Re(\boldsymbol{f}_n^H\mathbf{\Xi}_t\boldsymbol{f}) - \boldsymbol{f}_n^H\mathbf{\Xi}_t\boldsymbol{f}_n}{\boldsymbol{f}^H\mathbf{\Xi}_c\boldsymbol{f} + K\sigma_r^2\mathbf{w}^H\mathbf{w}} \\ \text{subject to} \quad & \|\mathbf{V}_k\boldsymbol{f}\|_2^2 \le P_k, \forall k, \\ & \xi\boldsymbol{f}^H\bar{\mathbf{R}}_u\boldsymbol{f} - 2\Re(\boldsymbol{f}_n^H\mathbf{R}_u\boldsymbol{f}) \le const., \forall u \end{aligned} \tag{18}$$

where $const. = -\xi K\sigma_c^2 - \boldsymbol{f}_n^H\mathbf{R}_u\boldsymbol{f}_n$ and $\boldsymbol{f}_n$ denotes the value in last iteration. Noticed that problem (18) can be tackled by Dinkelbach's algorithm according to the following Lemma.

Lemma 2: Let $\mathcal{X}$ be a convex set, $f(\mathbf{x})$ be a non-negative concave function over $\mathcal{X}$, and $g(\mathbf{x})$ be a convex function over $\mathcal{X}$. Then, the fractional programming (GFP) problem

$$\begin{aligned} \underset{\mathbf{x}}{\text{maximize}} \ & \frac{f(\mathbf{x})}{g(\mathbf{x})} \\ \text{subject to } & \mathbf{x} \in \mathcal{X}, \end{aligned} \tag{19}$$

can be solved via Dinkelbach's algorithm [26].

3. Update of phase shift matrix $\mathbf{\Phi}$

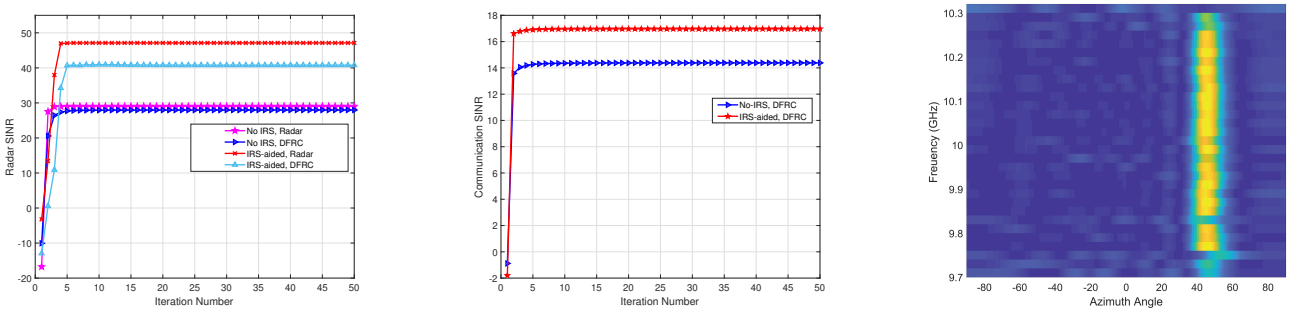

(a) (b) (c)

Figure 1. (a) Radar SINR versus number of iterations, (b) Communication SINR versus number of iterations, (c) Wideband transmit beampattern.

With the fixed t, $\mathbf{w}$ and $\mathbf{F}_k$, the corresponding optimization problem can be written as

$$\begin{aligned} &\underset{\boldsymbol{\phi}}{\text{maximize}} \ \frac{\bar{f}(\boldsymbol{\phi})}{\bar{g}(\boldsymbol{\phi})} \\ &\text{subject to } |\boldsymbol{\phi}(i)| = 1, \forall i \\ &\qquad \frac{q_u + 2\Re\{\boldsymbol{\phi}^H \mathbf{q}_u\} + \boldsymbol{\phi}^H \mathbf{Q}_u \boldsymbol{\phi}}{\bar{q}_u + 2\Re\{\boldsymbol{\phi}^H \bar{\mathbf{q}}_u\} + \boldsymbol{\phi}^H \bar{\mathbf{Q}}_u \boldsymbol{\phi} + K\sigma_c^2} \geq \xi, \forall u, \end{aligned} \tag{20}$$

where $\boldsymbol{\phi} = \text{diag}(\boldsymbol{\Phi})$, $\bar{f}(\boldsymbol{\phi})$ and $\bar{g}(\boldsymbol{\phi})$ are quartic over the variable $\boldsymbol{\phi}$. Hence, the auxiliary variable $\boldsymbol{\psi}$ is introduced to reformulate problem (19) as

$$\begin{aligned} &\underset{\boldsymbol{\phi},\boldsymbol{\psi}}{\text{maximize}} \ \bar{f}(\boldsymbol{\phi},\boldsymbol{\psi}) - \bar{\lambda}\bar{g}(\boldsymbol{\phi},\boldsymbol{\psi}) \\ &\text{subject to } \boldsymbol{\phi} = \boldsymbol{\psi} \\ &\qquad |\boldsymbol{\phi}(i)| = 1, |\boldsymbol{\psi}(i)| = 1, \forall i \\ &\qquad 2\Re(\mathbf{r}_u^H \boldsymbol{\phi}) \leq d_u, \forall u, \end{aligned} \tag{21}$$

where $\mathbf{r}_u = (\xi\boldsymbol{\phi}_t^H(\bar{\mathbf{Q}}_u - \eta_u\mathbf{I}) + \xi\bar{\mathbf{q}}_u^H - \mathbf{q}_u^H - \boldsymbol{\phi}_t^H\mathbf{Q}_u)^H$, η_u is the largest eigenvalue of $\bar{\mathbf{Q}}_u$, $d_u = \xi(\bar{q}_u + K\sigma_c^2 - 2\eta MN_m + \boldsymbol{\phi}_t^H\bar{\mathbf{Q}}_u\boldsymbol{\phi}_t) + \boldsymbol{\phi}_t^H\mathbf{Q}_u\boldsymbol{\phi}_t - q_u$, $\boldsymbol{\phi}_t$ denotes the current point of $\boldsymbol{\phi}$, $\bar{f}(\boldsymbol{\phi},\boldsymbol{\psi})$ and $\bar{g}(\boldsymbol{\phi},\boldsymbol{\psi})$ are quadratic over $\boldsymbol{\phi}$ and $\boldsymbol{\psi}$, respectively. Then, the augmented Lagrangian function of (21) is given by

$$\begin{aligned} \mathcal{L}(\boldsymbol{\phi},\boldsymbol{\psi},\mathbf{u},\mathbf{w},\rho) &= f(\boldsymbol{\phi},\boldsymbol{\psi},\bar{\lambda}) - \mathbf{u}^H(\boldsymbol{\phi}-\boldsymbol{\psi}) \\ &\quad - \frac{\rho}{2}\|\boldsymbol{\phi}-\boldsymbol{\psi}\|_2^2 - \sum_{u=1}^{U} w_u(2\Re(\mathbf{r}_u^H\boldsymbol{\phi}) - d_u), \end{aligned} \tag{22}$$

where $f(\boldsymbol{\phi},\boldsymbol{\psi},\bar{\lambda}) = \bar{f}(\boldsymbol{\phi},\boldsymbol{\psi}) - \bar{\lambda}\bar{g}(\boldsymbol{\phi},\boldsymbol{\psi})$, ρ is the penalty parameter, $\mathbf{u}$ and $\mathbf{w} \succeq \mathbf{0}$ denote the auxiliary variables. Based on above, ADMM-based update formulas are given by

$$\lambda^{(t+1)} = \frac{\bar{f}(\boldsymbol{\phi})}{\bar{g}(\boldsymbol{\phi})}, \tag{23a}$$

$$\boldsymbol{\phi}^{(t+1)} = \arg \max_{|\boldsymbol{\phi}|=1} \mathcal{L}(\lambda^{(t+1)}, \boldsymbol{\phi}, \boldsymbol{\psi}^{(t)}, \mathbf{u}^{(t)}, \mathbf{v}^{(t)}), \tag{23b}$$

$$\boldsymbol{\psi}^{(t+1)} = \arg \max_{|\boldsymbol{\psi}|=1} \mathcal{L}(\lambda^{(t+1)}, \boldsymbol{\phi}^{(t+1)}, \boldsymbol{\psi}, \mathbf{u}^{(t)}, \mathbf{v}^{(t)}), \tag{23c}$$

$$\mathbf{u}^{(t+1)} = \mathbf{u}^{(t)} + \rho_1(\boldsymbol{\phi}^{(t+1)} - \boldsymbol{\psi}^{(t+1)}), \tag{23d}$$

$$w_u^{(t+1)} = \text{Proj}_+(w_u^{(t)} - (2\Re(\mathbf{r}_u^H\boldsymbol{\phi}) - d_u)), \forall u. \tag{23e}$$

At each iteration of ADMM, the subproblems w.r.t phase-shift $\boldsymbol{\phi}$ and $\boldsymbol{\psi}$ can be solved by Riemannian steepest decent (RSD) algorithm [16]. Due to the space limitation, the RSD algorithm will be illustrated with details in the full version of this work.

4. *Update of auxiliary variable* t

For the given $\mathbf{w}$, $\mathbf{F}_k$ and $\boldsymbol{\Phi}$, the problem with respect to t is given by

$$\begin{aligned} &\underset{t}{\text{maximize}} \quad t \\ &\text{subject to} \quad \text{SINR}_u \geq t, \forall u. \end{aligned} \tag{24}$$

We can update it by

$$t = \max\{t_n, \arg\min_u \ \text{SINR}_u\}, \tag{25}$$

where t_n denotes the value of t at the last iteration.

IV. Numerical Experiments

Throughout the simulations, we assume both the DFBS and radar receiver are equipped with the ULA with $N_t = 10$ and $N_r = 8$ elements, respectively, and located at $[0, 0]$ in Cartesian plane. A single moving target is located at $[0, 5000]$. Two clutters is from $15°$ and $-25°$. We assume that IRS consists of $N_m = 30$ reflecting elements is deployed at $[2500, 2500]$ to assist the DFRC system. The central frequency of the wideband DFRC is 10 GHz and the subcarrier step-size is set as 20 MHz. Meanwhile, we set $K = 32$ and $U = 2$, respectively. The related element spacing for DFBS, radar receive and IRS are set according to the highest frequency, i.e., $d = c/2f_{max}$. The transmit power constraints at all subcarriers are set as identical, i.e., $P_1 = \cdots, = P_K = 10$. The beamforming matrices $\mathbf{F}_k$ and phase-shift matrices $\boldsymbol{\Phi}$ are initialized with the diagonal entries generated from a zero-mean Gaussian distribution. The maximum iteration for both inner-loop and out-loop are set as 50 times.

Fig.1(a) shows the achievable radar SINR versus the number of iterations. It is seen that the proposed algorithm converges within around 10 iterations. IRS-aided radar-only system can achieve the best performance due to the signal from both transmitter and IRS are align to the target direction. Meanwhile, comparing to the No-IRS DFRC, the proposed IRS-aided DFRC can provide more than 10 dB extra gain for radar performance.

Fig.1(b) demonstrates the achieved mininal communication SINR the number of iterations. Once again, the proposed algorithm can be convergent within around 10 iterations with respect to minimal communication SINR. Similarly, compared with No-IRS case, IRS-aided DFRC is superior with about 2.5 dB enhancement for the minimal communication SINR.

Fig.1(c) shows the wideband transmit beampattern of the dual-function transmitter. It is seen that the transmit energy is almost totally focused on the direction of IRS. This is because that we consider the higher gain for indirect link (i.e., IRS-aided channel) compared with direct link. Hence, we conclude that the proposed method can automatically align the transmit beam to the direction target or IRS.

V. Summary

In this paper, we consider utilizing IRS to assist the wideband OFDM-DFRC system in which both the LoS and NLoS paths from the DFBS to target/user are considered. To overcome the spatial wideband effect, the frequency-dependent transmit beamforming is devised. Specifically, we aim to design the radar receive filter, transmit active beamforming and phase-shift matrices (i.e., passive beamforming) to enhance the radar SINR and the minimal communication SINR among all users, simultaneously. Then, an alternating maximization (AM) based algorithm is developed to tackle the resulting problem. Simulation results shows that the proposed method can achieve satisfactory performance both in radar and communication.

Acknowledgment

This work was supported by the Luxembourg National Research Fund (FNR) through the SPRINGER Project, ref 12734677.

References

[1] M. Di Renzo, A. Zappone, M. Debbah, M.-S. Alouini, C. Yuen, J. de Rosny, and S. Tretyakov, "Smart radio environments empowered by reconfigurable intelligent surfaces: How it works, state of research, and the road ahead," *IEEE Journal on Selected Areas in Communications*, vol. 38, no. 11, pp. 2450–2525, 2020.

[2] Q. Wu and R. Zhang, "Towards smart and reconfigurable environment: Intelligent reflecting surface aided wireless network," *IEEE Communications Magazine*, vol. 58, no. 1, pp. 106–112, 2020.

[3] J. A. Hodge, K. V. Mishra, and A. I. Zaghloul, "Intelligent time-varying metasurface transceiver for index modulation in 6G wireless networks," *IEEE Antennas and Wireless Propagation Letters*, vol. 19, no. 11, pp. 1891–1895, 2020.

[4] Q. Wu and R. Zhang, "Intelligent reflecting surface enhanced wireless network via joint active and passive beamforming," *IEEE Transactions on Wireless Communications*, vol. 18, no. 11, pp. 5394–5409, 2019.

[5] C. Huang, A. Zappone, G. C. Alexandropoulos, M. Debbah, and C. Yuen, "Reconfigurable intelligent surfaces for energy efficiency in wireless communication," *IEEE Transactions on Wireless Communications*, vol. 18, no. 8, pp. 4157–4170, 2019.

[6] C. Pan, H. Ren, K. Wang, W. Xu, M. Elkashlan, A. Nallanathan, and L. Hanzo, "Multicell MIMO communications relying on intelligent reflecting surfaces," *IEEE Transactions on Wireless Communications*, vol. 19, no. 8, pp. 5218–5233, 2020.

[7] M. F. Ahmed, K. P. Rajput, N. Venkategowda, K. V. Mishra, and A. K. Jagannatham, "Joint transmit and reflective beamformer design for secure estimation in IRS-aided WSNs," *IEEE Signal Processing Letters*, pp. 1–1, 2022.

[8] Z. Esmaeilbeig, K. V. Mishra, and M. Soltanalian, "IRS-aided radar: Enhanced target parameter estimation via intelligent reflecting surfaces," 2021.

[9] S. Buzzi, E. Grossi, M. Lops, and L. Venturino, "Radar target detection aided by reconfigurable intelligent surfaces," *IEEE Signal Processing Letters*, vol. 28, pp. 1315–1319, 2021.

[10] K. V. Mishra, A. Chattopadhyay, S. S. Acharjee, and A. P. Petropulu, "OptM3Sec: Optimizing multicast IRS-aided multiantenna DFRC secrecy channel with multiple eavesdroppers," *ArXiv*, vol. abs/2201.09436, 2022.

[11] X. Wang, Z. Fei, Z. Zheng, and J. Guo, "Joint waveform design and passive beamforming for RIS-assisted dual-functional radar-communication system," *IEEE Transactions on Vehicular Technology*, vol. 70, no. 5, pp. 5131–5136, 2021.

[12] J. Liu, X. Qian, and M. Di Renzo, "Interference analysis in reconfigurable intelligent surface-assisted multiple-input multiple-output systems," in *IEEE International Conference on Acoustics, Speech and Signal Processing (ICASSP)*, 2021, pp. 8067–8071.

[13] M. Najafi, V. Jamali, R. Schober, and H. V. Poor, "Physics-based modeling and scalable optimization of large intelligent reflecting surfaces," *IEEE Transactions on Communications*, vol. 69, no. 4, pp. 2673–2691, 2021.

[14] Z. Zhou, N. Ge, Z. Wang, and L. Hanzo, "Joint transmit precoding and reconfigurable intelligent surface phase adjustment: A decomposition-aided channel estimation approach," *IEEE Transactions on Communications*, vol. 69, no. 2, pp. 1228–1243, 2021.

[15] A. Elzanaty, A. Guerra, F. Guidi, and M.-S. Alouini, "Reconfigurable intelligent surfaces for localization: Position and orientation error bounds," *IEEE Transactions on Signal Processing*, vol. 69, pp. 5386–5402, 2021.

[16] Z. Li, M. Hua, Q. Wang, and Q. Song, "Weighted sum-rate maximization for multi-IRS aided cooperative transmission," *IEEE Wireless Communications Letters*, vol. 9, no. 10, pp. 1620–1624, 2020.

[17] W. Lu, B. Deng, Q. Fang, X. Wen, and S. Peng, "Intelligent reflecting surface-enhanced target detection in MIMO radar," *IEEE Sensors Letters*, vol. 5, no. 2, pp. 1–4, 2021.

[18] W. Lu, Q. Lin, N. Song, Q. Fang, X. Hua, and B. Deng, "Target detection in intelligent reflecting surface aided distributed MIMO radar systems," *IEEE Sensors Letters*, vol. 5, no. 3, pp. 1–4, 2021.

[19] A. Aubry, A. De Maio, and M. Rosamilia, "Reconfigurable intelligent surfaces for N-LOS radar surveillance," *IEEE Transactions on Vehicular Technology*, vol. 70, no. 10, pp. 10 735–10 749, 2021.

[20] K. V. Mishra, B. Shankar M. R., V. Koivunen, B. Ottersten, and S. A. Vorobyov, "Toward millimeter-wave joint radar communications: A signal processing perspective," *IEEE Signal Processing Magazine*, vol. 36, no. 5, pp. 100–114, 2019.

[21] T. Wei, L. Wu, and B. Shankar M. R., "Joint waveform and precoding design for coexistence of MIMO radar and MU-MISO communication," *IET Signal Processing*, pp. 1–13, 2022.

[22] Z.-M. Jiang, M. Rihan, P. Zhang, L. Huang, Q. Deng, J. Zhang, and E. M. Mohamed, "Intelligent reflecting surface aided dual-function radar and communication system," *IEEE Systems Journal*, pp. 1–12, 2021.

[23] R. S. P. Sankar, B. Deepak, and S. P. Chepuri, "Joint communication and radar sensing with reconfigurable intelligent surfaces," *arXiv*, 2021.

[24] M. Wang, F. Gao, S. Jin, and H. Lin, "An overview of enhanced massive mimo with array signal processing techniques," *IEEE Journal of Selected Topics in Signal Processing*, vol. 13, no. 5, pp. 886–901, 2019.

[25] Z.-q. Luo, W.-k. Ma, A. M.-c. So, Y. Ye, and S. Zhang, "Semidefinite relaxation of quadratic optimization problems," *IEEE Signal Processing Magazine*, vol. 27, no. 3, pp. 20–34, 2010.

[26] A. Aubry, A. De Maio, and M. M. Naghsh, "Optimizing radar waveform and doppler filter bank via generalized fractional programming," *IEEE Journal of Selected Topics in Signal Processing*, vol. 9, no. 8, pp. 1387–1399, 2015.